Electronic structure of radially deformed BN and BC_3 nanotubes

Yong-Hyun Kim,[1,2] K. J. Chang,[1,2] and S. G. Louie[1,3]
[1]*School of Physics, Korea Institute for Advanced Study, Seoul 130-012, Korea*
[2]*Department of Physics, Korea Advanced Institute for Science and Technology, Taejon 305-701, Korea*
[3]*Department of Physics, University of California, Berkeley, California 94720*
and Materials Sciences Divison, Lawrence Berkeley National Laboratory, Berkeley, California 94720
(Received 4 October 2000; revised manuscript received 15 February 2001; published 20 April 2001)

We investigate the band-gap modification by radial deformation in BN and BC_3 nanotubes through first-principles pseudopotential density-functional calculations. In zigzag BN nanotubes, radial deformations that give rise to transverse pressures of about 10 GPa decrease the gap from 5 to 2 eV, allowing for optical applications in the visible range. When armchair BC_3 nanotubes with the gap of about 0.5 eV are collapsed down to the interlayer distance of 3.5 Å, a gap closure occurs due to the lowering of the unoccupied π band. On the other hand, the band gaps of armchair BN and zigzag BC_3 nanotubes are found to be insensitive to radial deformations. This different behavior between zigzag and armchair nanotubes is attributed to the different characteristics of states near the gap.

DOI: 10.1103/PhysRevB.63.205408 PACS number(s): 61.48.+c, 71.20.Tx, 71.20.Nr, 73.22.−f

Carbon nanotubes that consist of only carbon atoms can be thought as a single layer of graphite that is wrapped into a cylinder.[1] The electronic structure of a perfect C nanotube is known to be either metallic or semiconducting, depending on tube diameter and wrapping angle.[2–5] The mean diameter of C nanotubes can be controlled by varying target temperature in synthesis.[6] However, a broad distribution of nanotube diameters still exists, and to date it seems difficult to control in a practical way, precisely the tube diameter and helicity for nanosized electronic and photonic devices. Although the cylindrical form of nanotubes is extremely rigid to distortions along the tube axis, it is very flexible to those perpendicular to the axis. In addition, the electronic properties of carbon nanotubes are sensitively modified by structural changes such as twisting and topological defects.[7,8] Very recent theoretical calculations proposed that it is possible to control with relative ease the electronic structure of C nanotubes by flattening deformations, which can be imposed by transverse pressures or locally by electrode contacts.[9,10] Flattening deformations induce the band-gap modification such as opening and closure, thus, locally created energy barriers can make quantum dots or wires in C nanotubes.

The existence of BN, BC_3, and BC_2N nanotubes was theoretically proposed,[11–14] and experimental realizations have been made for BN and BC_3 nanotubes as well as composite $B_xC_yN_z$ nanotubes including signature of BC_2N.[15–17] Due to the ionic origin of the band gap, BN nanotubes with diameters larger than 9.5 Å [which corresponds to the diameter of the (12,0) tube] have a very stable quasiparticle gap of about 5.5 eV, almost independent of tube diameter, helicity, and wall-wall interactions. As the C composition increases in $B_xC_yN_z$ nanotubes, the calculated band gap within the local-density-functional approximation (LDA) generally decreases, to 2.0 and 0.5 eV, for BC_2N and BC_3 nanotubes, respectively. Thus, the synthesis of composite $B_xC_yN_z$ nanotubes would make possible applications for electronic and photonic devices with a variety of electronic properties.[18] However, a helicity selection was observed in both multiwall and single-wall BN nanotubes,[17] while C nanotubes exhibit random helicities. Using molecular-dynamics simulations, Blase and co-workers attributed this helicity selection to the greater stability of B-N bonds, as compared to B-B and N-N bonds.[19] In view of such difficulties in selective growth of nanotubes, band-gap engineering using simple flattening deformation, combined with the lack of chemical reactivity,[20] is a promising means for device applications of B- and C-based nanotubes.

In this paper, we study the electronic structure of collapsed BN and BC_3 nanotubes through first-principles pseudopotential density-functional calculations. In the zigzag (9,0) BN tube, the LDA band gap varies from 3.5 to 1.0 eV with increasing severity of flattening deformation, while the band gap of armchair BN tubes is little affected. Similar deformations induce a semiconductor-metal transition in armchair BC_3 nanotubes, which have relatively small gaps. However, the electronic properties of zigzag BC_3 nanotubes are insensitive to radial deformation, similar to the case of armchair BN tubes. Such distinct modifications by deformation should allow tuning of band gaps for device applications.

To investigate the effect of radial deformations on the electronic structure of BN and BC_3 nanotubes, we perform first-principles pseudopotential calculations within the LDA. *Ab initio* norm-conserving pseudopotentials are generated by the scheme of Troullier and Martins,[21] and transformed into the Kleinman-Bylander separable form.[22] The Ceperley-Alder exchange and correlation potential[23] is used. The wave functions are expanded in a plane-wave basis set with a kinetic-energy cutoff of 36 Ry, which ensures the convergence of band energy differences to within 0.05 eV. The LDA calculations are carried out for tetragonal supercells with atoms on neighboring tubes at distances larger than 6 Å away. We calculate the Hellmann-Feynman forces and relax ionic positions using the quasi-Newton method[24] until the collapsed geometry is fully optimized. During relaxation, we impose the constraint that atoms are only allowed to move between two infinite barriers, the separation of which gives the interlayer distance d of the collapsed tube. Before gener-

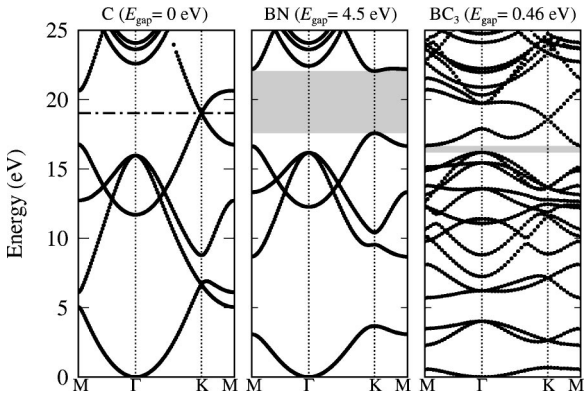

FIG. 1. The LDA band structures for BN and BC_3 sheets are compared with that for a single graphite sheet in the hexagonal Brillouin zone. The dot-dashed line and shaded regions denote the Fermi level and band gap, respectively.

ating collapsed nanotubes, we calculate the equilibrium bond distances. For a graphitic layer of BN, the B-N bond distance is calculated to be 1.45 Å, while the B-C and C-C bond distances in a single BC_3 sheet are 1.55 and 1.41 Å, respectively. We find similar bond distances in collapsed BN and BC_3 nanotubes.

The band structure of a nanotube basically stems from the **k**-space energy surface of a graphitic sheet through band-folding effect. Thus, the band gap of the corresponding sheet is the limiting value of band gaps of nanotubes, as tube diameter increases. In Fig. 1, the LDA band structures of BN and BC_3 single layers are compared with that for a graphite sheet near the Fermi level. A graphite sheet has a hexagonal primitive cell with two C basis atoms at (0,0) and $(\frac{1}{3},\frac{1}{3})$ in units of the lattice vectors. In a π-orbital approximation,[5] with only the p_z orbitals of the basis atoms included, two energy levels characterized by π and π^* are degenerate at the Fermi level. The Fermi point is positioned at the *K* point in the two-dimensional hexagonal Brillouin zone. Since the two basis atoms in the primitive cell are identical, the charge densities for the π and π^* states are equally distributed around the basis atoms. The π and π^* states are composed of a different combination of the p_z orbitals, corresponding to $1/\sqrt{2}(1,1)$ and $1/\sqrt{2}(1,-1)$, respectively, which we will simply denote as $(1,1)$ and $(1,-1)$ in the discussion below.[10]

In a single BN sheet, the B-N bond length of 1.45 Å is slightly larger than the C-C bond length in a graphene. Because of the ionic B-N bond, the degeneracy at the Fermi level is removed. A large LDA direct gap of 4.5 eV is found at the *K* point, as compared to the measured gap of near 5.5 eV. In supercell calculations, when the layer-layer distance is at about 6 Å, we find however an indirect gap due to layer-layer interactions.[12] It is noted that the π state mostly consists of p_z orbitals around the N atoms, while the π^* state is composed of p_z orbitals distributed around the B atoms; thus, the π and π^* states are expressed as (0,1) and (1,0), respectively. Because the electron affinity of the N atom is larger, the (0,1) state has lower energy than the (1,0) state.

For a BC_3 sheet, we adopt the geometry proposed by previous theoretical calculations,[13] where six C atoms form a hexagon surrounded by six B atoms. Thus, C-C and B-C bonds are symmetrically arranged with respect to the hexagon center, while B-B bonds are excluded. We find linearly dispersing π and π^* bands crossing at the *K* point, similar to the graphite sheet. However, because of the lack of one valence electron on each B atom compared to carbon, the π state is completely unoccupied, as shown in Fig. 1, becoming the lowest-unoccupied-molecular-orbital (LUMO) state, which has the charge distribution mainly at the B-C bonds. The highest-occupied-molecular-orbital (HOMO) state is characterized by the σ bonding between the constituent atoms.[25,26] We find an indirect band gap of 0.46 eV from Γ to *M*. Although a monolayer has a finite band gap, a layered structure of bulk BC_3 is known to have band overlaps and a high conductivity due to layer-layer interactions.[26]

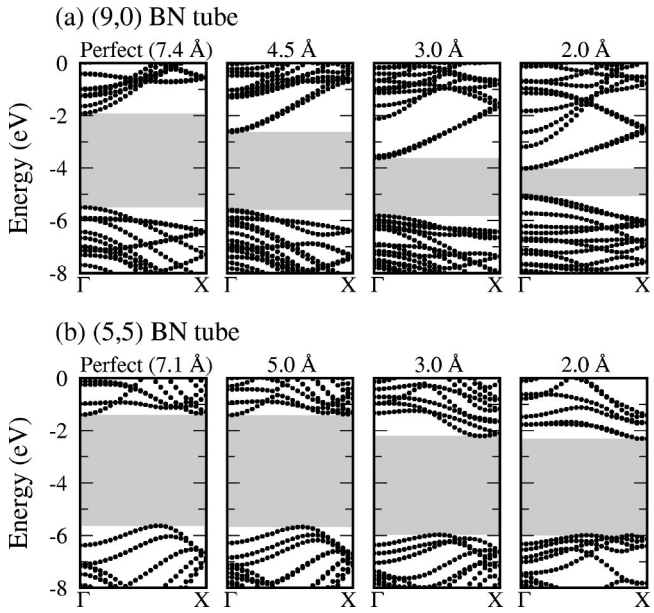

FIG. 2. The variations of the band gaps with flattening deformation in (a) (9,0) and (b) (5,5) BN nanotubes. The shaded regions denote the band gaps and the number indicates the separation (d) of the two opposing faces of the flattened tubes.

It is known that BN and BC_3 nanotubes with large diameters are semiconductors with band gaps of about 5.5 and 0.5 eV, respectively,[11–13] while insulating C nanotubes become metallic with increasing diameter, independent of the wrapping index.[27] In BN tubes with diameters less than 9.5 Å, however, previous tight-binding calculations showed that as tube diameter decreases, the band gap of the zigzag tubes decreases more rapidly, as compared to that of the armchair tubes.[11] Since the curvature of tubes is effectively enhanced by a flattening deformation, the sensitivity of band gap to flattening deformation is expected to be higher in zigzag tubes. The band structures of the zigzag (9,0) and armchair (5,5) BN tubes are plotted and compared for various flattening deformations in Fig. 2. In the plot, for each deformed nanotube, the band energies are given with respect to the vacuum level, which is defined as the total local potential evaluated in the vacuum region of the supercell in the calculation. As expected, for the (9,0) nanotube, the band gap is reduced from 3.5 to 1.0 eV as the tube is flattened from *d*

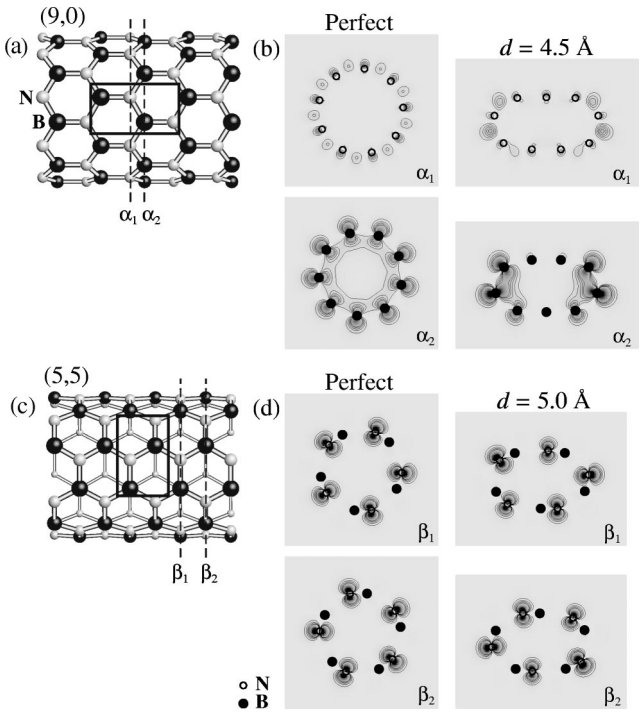

FIG. 3. Ball-and-stick models for (a) (9,0) and (c) (5,5) BN nanotubes. The rectangular boxes are the smallest building blocks to construct the nanotube lattices by repeating along the circumferential direction. (b) Charge-density contours for the LUMO states in the perfect (left panel) and flattened (right panel) (9,0) tubes in the cross sections, α_1 and α_2. (d) Charge-density contours for the HOMO states in the perfect (left panel) and flattened (right panel) (5,5) tubes in the cross sections, β_1 and β_2.

$=7.4$ to $d=2.0$ Å, varying almost linearly with the interlayer distance d. However, a gap closure does not occur and a direct gap is found at the Γ point in all the collapsed tubes considered. To deform BN nanotubes to $d=3.0$ Å, a transverse pressure of about 10 GPa is needed, as estimated from the total-energy variation with deformation. For moderate deformations down to near the van der Waals interlayer spacing, the gap is found to be about 2 eV. Since zigzag tubes with large diameters have a gap of ~ 5 eV, flattening deformation allows the tuning of energy gap in the range of $1-5$ eV.

In zigzag nanotubes, the smallest building block in constructing the nanotube lattice is a rectangular cell containing two B and two N atoms, as shown in Fig. 3(a), which is twice as large as the unit cell of an isolated flat sheet. Repeating the rectangular cell along the circumferential direction gives rise to the conventional primitive cell of the zigzag nanotube. An analysis of wave functions in the rectangular box is important in understanding the wave functions of the whole nanotube.[10] When a graphitic BN sheet is rolled up, the wave vectors (k_x) perpendicular to the tube axis are quantized such as $k_x=2\pi q/L$, where L is the circumference of the tube and q is an integer. In the perfect (9,0) BN tube, the LUMO state corresponds to the $q=0$ state. Since the $q=0$ state is represented by the wave function $(1,0,-1,0)$ for the four consecutive atoms (B-N-B-N) in the rectangular cell in Fig. 3(a), only the B atoms have p_z orbitals. In fact, we find that appreciable charge densities are accumulated at the B atoms, while very little charges at the N atoms, as illustrated in Fig. 3(b). When the tube is flattened, the $q=0$ band-folded state is mixed with a subband state in the conduction band, causing a charge transfer from the flattened layers to the curved regions. Then, an overlap of the charge densities is induced in the curved regions. Because of the formation of weak bonds between the B atoms in the curved regions, the conduction-band minimum state decreases under flattening deformation. Similar behavior was also found in zigzag carbon nanotubes, where the singly degenerate state decreases due to the enhanced accumulation of charge densities in the curved regions.[9,10]

The armchair nanotube lattice can also be constructed by repeating the same building block as that in zigzag tubes, but now it is rotated by 90° with respect to the tube axis. For the consecutive B-N-B-N atoms in a rectangular cell, the LUMO state (π^*) is represented as $(1,0,-1,0)$, similar to the $q=0$ state in the (9,0) tube, while the HOMO state (π) is represented as $(0,1,0,-1)$. The results indicate that the p_z orbitals reside only at one type of atoms for these states. Figure 3(d) shows the charge densities of the HOMO states for the perfect and the flattened tubes, indicating that this state maintains the characteristics of the $(0,1,0,-1)$ wave function, with almost equal weights inside and outside the tube. A charge transfer from the flattened layers to the curved regions is not found, in contrast to the case of zigzag tubes. This is due to the large distance between same species along the circumference, which makes it unfavorable for an overlap of charge densities in the curved regions. As the (5,5) BN tube is collapsed, the free-electronlike tubule conduction band,[12] which is the LUMO state at the initial stage of flattening, moves to higher energies, while a new π^* subband appears as the LUMO state near the X point, as shown in Fig. 2(b). Nevertheless, for small deformations down to $d=5.0$ Å, the band gap is little affected by flattening deformation. However, for d less than an interlayer spacing of 3.35 Å, the gap suddenly decreases by 0.5 eV due to interactions between the two facing layers of the collapsed tube. This situation is similar to the case of collapsed armchair C nanotubes. When armchair C nanotubes undergo flattening deformation that breaks all mirror symmetries of the tube, the broken symmetry induces a mixing of two linear bands, which are even and odd under mirror symmetry operations, resulting in a gap opening. In this case, very small gaps (less than 10 meV) are induced for flattening deformations of $d \geqslant 4.0$ Å, while the gap increases to about 0.1 eV as layer-layer interactions become significant at $d=3.35$ Å.[9,10]

In previous tight-binding calculations for BC_3 nanotubes, the band gap of perfect zigzag tubes was found to decrease as tube diameter decreases, while armchair (n,n) $(n=3,4,5)$ tubes have an almost constant gap independent of their diameters.[13] Thus, one might naively expect a band gap closure to be more likely to occur in zigzag BC_3 tubules under flattening deformation. In our LDA calculations for collapsed (4,0) and (3,3) BC_3 nanotubes, we only find a gap closure in the armchair tube, as shown in Fig. 4. This peculiar behavior results from the fact that BC_3 tubes have both the π and π^* bands above the Fermi level, while the top of

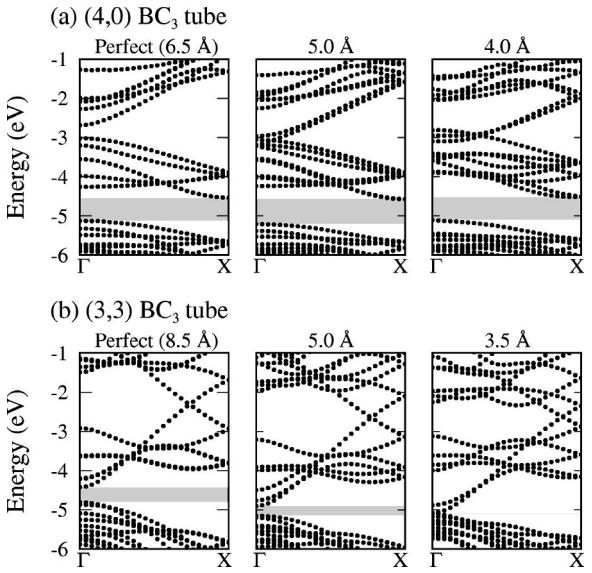

FIG. 4. Variations of the band gaps with flattening deformation in (a) (4,0) and (b) (3,3) BC_3 nanotubes. The shaded regions denote the band gaps and the number indicates the separation (d) of the two opposing faces in the flattened tubes.

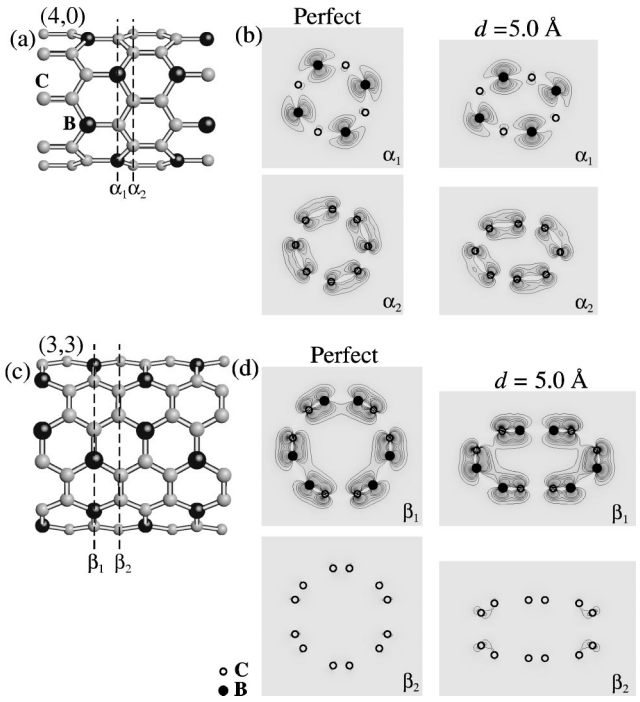

FIG. 5. Ball-and-stick models of (a) (4,0) and (c) (3,3) BC_3 nanotubes. (b) Charge-density contours for the LUMO states in the perfect ($d=6.5$ Å) and flattened ($d=5.0$ Å) (4,0) BC_3 tubes in the cross sections, α_1 and α_2. (d) Charge-density contours for the LUMO states in the perfect ($d=8.5$ Å) and flattened ($d=5.0$ Å) (3,3) BC_3 tubes in the cross sections, β_1 and β_2.

the valence bands has σ character. The folded bands of the unoccupied π band of a single BC_3 sheet have a bandwidth of about 1.5 eV and are located just above the band gap. A higher energy gap between the π and π^* bands, which is analogous to real gaps in C nanotubes, is seen at the Γ point in the zigzag tube, and decreases under flattening deformation, similar to collapsed C nanotubes. Such a gap in the conduction-band complex is in fact closed for an interlayer spacing between 5 and 6 Å. However, as the zigzag tube is flattened, the π band complex width increases slightly, with a small upward movement at the Γ point. Figure 5(b) shows the charge densities for the lowest π conduction-band state located at the X point, which are mostly distributed at the zigzag B-C bonds, with the π orbitals at the B atoms. Since flattening deformation does not disturb this charge distribution, the lowest conduction-band state is insensitive to deformation. In addition, the highest valence-band state with σ character is also unaffected by deformation. Thus, the fundamental gap of about 0.6 eV from Γ to X for the (4,0) BC_3 tube is almost independent of flattening deformation.

On the other hand, for the armchair BC_3 tube, the π and π^* conduction bands cross each other near 2/3 of the distance from Γ to X on the Γ-X line. When one mirror symmetry is preserved during deformation, the degeneracy still remains at the crossing point. But, the crossing point of the π and π^* bands moves closer to the X point as flattening deformation is enhanced, indicating that the movements of the π and π^* bands are opposite with π bands lowering in energy. In collapsed armchair C nanotubes, the crossing point of π and π^* was found to move to the Γ point. Figure 5(d) shows the charge densities for the lowest conduction-band state located at the Γ point, which are accumulated at the B-C bonds normal to the tube axis. In collapsed armchair tubes, we find that the p_z orbitals on both the B and C atoms are more noticeably overlapped in the curved regions. Because of the weak bonds induced by the overlap of p_z orbitals, the lowest conduction-band state is lowered. We find a gap closure when the tube is flattened down to $d=3.5$ Å for the (3,3) BC_3 tube.

In device applications, the preferentially grown zigzag BN nanotubes would be promising optical materials in nanometric size, because the band gaps are tunable with flattening deformation. Depending on the severity of flattening, the energy gaps range from ultraviolet to infrared. On this basis, we consider the effect of localized deformations in zigzag BN nanotubes, where a small deformed region is sandwiched between two longer and perfectly shaped tubes. From our LDA calculations, we find band offsets of about 0.4 and 2.1 eV for the valence and conduction bands, respectively, for the locally deformed tube with $d=2.0$ Å, as shown in Fig. 6. This band diagram is quite similar to that of the double het-

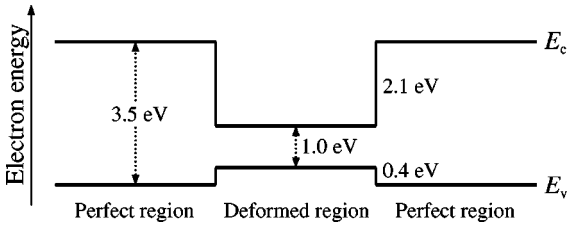

FIG. 6. The band diagram for a (9,0) BN nanotube device, where a locally deformed tube ($d=2.0$ Å) is sandwiched between two perfect tubes. Here E_v and E_c denote the valence-band maximum and conduction-band minimum states, respectively.

erostructure laser diode,[28] suggesting that the locally deformed tube may act as an optically active region.

In conclusion, we have performed first-principles pseudopotential density-functional calculations on BN and BC_3 nanotubes under flattening deformation. A pressure of about 10 GPa is needed to collapse the nanotubes down to a van der Waals interlayer spacing. We find the possibility of band-gap tuning in the range of $1-5$ eV in zigzag BN nanotubes, which gives rise to potentially useful variations in device applications. In BC_3 nanotubes, because of an overall reduction in the number of electrons per formula unit, the variation of the fundamental band gap with deformation is very different from those in both C and BN nanotubes. We find that flattening deformation induces a semiconductor-metal transition in armchair BC_3 nanotubes. In both armchair BN and zigzag BC_3 nanotubes, the band gap is insensitive to flattening deformation.

We thank Y.-G. Jin for his helpful discussions. This work was supported by the MOST and the QSRC at Dong-Kuk University. S.G.L. acknowledges the support of NSF Grant No. DMR-00-87088 and the director, Office of Energy Research, Office of Basic Energy Sciences, Materials Sciences Division of the U.S. Department of Energy under Contract No. DE-AC03-76SF00098.

[1] S. Iijima, Nature (London) **354**, 56 (1991).
[2] J.W. Mintmire, B.I. Dunlap, and C.T. White, Phys. Rev. Lett. **68**, 631 (1992).
[3] N. Hamada, S. Sawada, and A. Oshiyama, Phys. Rev. Lett. **68**, 1579 (1992).
[4] R. Saito, M. Fujita, G. Dresselhaus, and M.S. Dresselhaus, Appl. Phys. Lett. **60**, 2204 (1992).
[5] M. S. Dresselhaus, G. Dresselhaus, and P. C. Eklund, *Science of Fullerenes and Carbon Nanotubes* (Academic, San Diego, 1996); R. Saito, G. Dresselhaus, and M. S. Dresselhaus, *Physical Properties of Carbon Nanotubes* (Imperial College, London, 1998).
[6] S. Bandow, S. Asaka, Y. Saito, A.M. Rao, L. Grigorian, E. Richter, and P.C. Eklund, Phys. Rev. Lett. **80**, 3779 (1998).
[7] C.L. Kane and E.J. Mele, Phys. Rev. Lett. **78**, 1932 (1997).
[8] V.H. Crespi, M.L. Cohen, and A. Rubio, Phys. Rev. Lett. **79**, 2093 (1997).
[9] C.-J. Park, Y.-H. Kim, and K.J. Chang, Phys. Rev. B **60**, 10 656 (1999).
[10] Y.-H. Kim, C.-J. Park, and K.J. Chang, J. Korean Phys. Soc. **37**, 85 (2000).
[11] A. Rubio, J.L. Corkill, and M.L. Cohen, Phys. Rev. B **49**, 5081 (1994).
[12] X. Blase, A. Rubio, S.G. Louie, and M.L. Cohen, Phys. Rev. B **51**, 6868 (1995).
[13] Y. Miyamoto, A. Rubio, S.G. Louie, and M.L. Cohen, Phys. Rev. B **50**, 18 360 (1994).
[14] Y. Miyamoto, A. Rubio, M.L. Cohen, and S.G. Louie, Phys. Rev. B **50**, 4976 (1994).
[15] Z. Weng-Sieh, K. Cherrey, N.G. Chopra, X. Blase, Y. Miyamoto, A. Rubio, M.L. Cohen, S.G. Louie, A. Zettl, and R. Gronsky, Phys. Rev. B **51**, 11 229 (1995).
[16] N.G. Chopra, R.J. Luyken, K. Cherrey, V.H. Crespi, M.L. Cohen, S.G. Louie, and A. Zettl, Science **269**, 966 (1995).
[17] A. Loiseau, F. Willaime, N. Demoncy, G. Hug, and H. Pascard, Phys. Rev. Lett. **76**, 4737 (1996).
[18] X. Blase, J.-C. Charlier, A. De Vita, and R. Car, Appl. Phys. Lett. **70**, 197 (1997).
[19] X. Blase, A. De Vita, J.-C. Charlier, and R. Car, Phys. Rev. Lett. **80**, 1666 (1998).
[20] A. Rubio, Y. Miyamoto, X. Blase, M.L. Cohen, and S.G. Louie, Phys. Rev. B **53**, 4023 (1996).
[21] N. Troullier and J.L. Martins, Phys. Rev. B **43**, 1993 (1991).
[22] L. Kleinman and D.M. Bylander, Phys. Rev. Lett. **48**, 1425 (1982).
[23] D.M. Ceperley and B.J. Alder, Phys. Rev. Lett. **45**, 566 (1980).
[24] B.G. Pfrommer, M. Côté, S.G. Louie, and M.L. Cohen, J. Comput. Phys. **131**, 233 (1997).
[25] R.M. Wentzcovitch, M.L. Cohen, S.G. Louie, and D. Tománek, Solid State Commun. **67**, 515 (1988).
[26] D. Tománek, R.M. Wentzcovitch, S.G. Louie, and M.L. Cohen, Phys. Rev. B **37**, 3134 (1988).
[27] C.T. White, D.H. Robertson, and J.W. Mintmire, Phys. Rev. B **47**, 5485 (1993).
[28] L. A. Coldren and S. W. Corzine, *Diode Lasers and Photonic Integrated Circuits* (Wiley, New York, 1995).